Available online at www.sciencedirect.com

ScienceDirect

MATTER AND RADIATION AT EXTREMES

Matter and Radiation at Extremes 3 (2018) 85–93

www.journals.elsevier.com/matter-and-radiation-at-extremes

Research Article

Warm dense matter research at HIAF

Rui Cheng [a,*], Yu Lei [a,c], Xianming Zhou [a,c], Yuyu Wang [a], Yanhong Chen [a], Yongtao Zhao [a,b], Jieru Ren [b], Lina Sheng [a], Jiancheng Yang [a], Zimin Zhang [a], Yingchao Du [d], Wei Gai [e], Xinwen Ma [a], Guoqing Xiao [a,**]

[a] *Institute of Modern Physics, Chinese Academy of Sciences, Lanzhou 730000, China*
[b] *School of Science, Xi'an Jiaotong University, Xi'an 710049, China*
[c] *University of Chinese Academy of Sciences, Beijing 100049, China*
[d] *Department of Engineering Physics, Tsinghua University, Beijing 100084, China*
[e] *Argonne National Lab, Argonne, IL 60439, USA*

Received 15 June 2017; revised 31 October 2017; accepted 9 November 2017
Available online 30 December 2017

Abstract

The research activities on warm dense matter driven by intense heavy ion beams at the new project High Intensity heavy-ion Accelerator Facility (HIAF) are presented. The ion beam parameters and the simulated accessible state of matter at HIAF are introduced, respectively. The progresses of the developed diagnostics for warm dense matter research including high energy electron radiography, multiple-channel pyrometer, in-situ energy loss and charge state of ion detector are briefly introduced.

PACS Codes: 34.50.Bw; 94.20.Fg; 52.40.Mj; 87.59.B-; 41.75.Lx

Keywords: Warm dense matter; Intense heavy ion beams; HIAF; Electron radiography

1. Introduction

Warm Dense Matter (WDM), an intermediate state of matter between solid and plasma, has a density of the same order of magnitude as solid (typically 0.01−100 g/cm^3), a temperature on the order of a few eV (typically 1−100 eV) and a pressure from ambient to some Mbar. It exists in the lower-temperature portion of the high energy density regime [1]. In this state, the particles are strongly coupled. This means that the energy of the interaction between electrons and nuclei and the kinetic energy of electrons are of the same magnitude. Under the condition of WDM, the assumptions of both condensed matter theory and ideal-plasma theory break down, while the quantum mechanics, particle correlations and electric forces all become important. WDM is expected in the cores of large planets [2], e.g. Jupiter, in the path to inertial confinement fusion [3] and in nuclear explosion. It attracted more and more attention because of its importance and the accessibility to expected experiments.

The intense heavy-ion-beam-driven WDM is unique, with the advantages of large sample size of any target material, homogeneous physical condition, good reproducibility, high repetition rate, flexibility of isochoric heating of material at high density and shock compression at very low entropy [4–6]. It provides scientists with a novel, very efficient solution to study WDM physics besides the high power laser and pulsed power devices like Z-pinch [7–14].

However, to investigate the WDM physics by heavy-ion beams is very difficult, and a strongly-bunched, well-focused

* Corresponding author.
** Corresponding author.
E-mail addresses: chengrui@impcas.ac.cn (R. Cheng), xiaogq@impcas.ac.cn (G.Q. Xiao).

https://doi.org/10.1016/j.mre.2017.11.001
2468-080X/

and high-intensity energetic ion beam is a big challenge for the current accelerator technology. In order to improve the research of WDM driven by intense heavy-ion-beam, the accelerator complexes in the major accelerator laboratories and institutions in the world have been upgraded in the last few decades [15−24], i.e., the Facility for Antiprotons and Ion Research (FAIR) in Germany and NCDX-II at Lawrence Berkeley National Laboratory in USA, as well as the new project, High Intensity heavy ion Accelerator Facility (HIAF) in China.

The HIAF project was proposed by the Institute of Modern Physics (IMP), Chinese Academy of Sciences, and was selected as one of the 16 priority national projects for sciences and technology for the 12th 5-Year-Plan in China. In December 2015, the HIAF project was officially approved by Chinese government. Now the technical design was finished and the civil construction has started to develop. The intense heavy-ion-beam-driven WMD is one of the important research topics in HIAF project. A specially designed experimental terminal will be located at the high energy external target station, where $^{238}U^{34+}$ ions with an energy of hundreds of MeV/u, intensity of ~10^{11} ppp (~10^{12} ppp for the next upgrade in phase-II), a bunch length of 50−150 ns and a beam spot of ~1 mm which is strongly focused by the Final Focus Lens (FFL) system can be applied.

In this paper, the main parameters of HIAF and the related research activities for WDM are introduced. We present the new opportunities for EOS, critical point of metals, phase transition and hydrodynamic process, as well as ion-WDM interaction which can be experimentally investigated based on the HIAF project.

2. Introduction of HIAF and the beam generated WDM

The HIAF complex, whose schematic view is shown in Fig. 1, consists of a superconductive electronic cyclotron resonance (SECR) ion source, an ion-Linac (iLinac), a Booster Ring (BRing), a radioactive beam line of fragmentation type, a Spectrometer Ring (SRing), a Merge Ring (MRing), and different experimental terminals at low-, intermediate- and high-energy ends, as well as setups for in-ring experiments [25,26]. An electron cooler will be installed at BRing and a low-emitted and well compressed pulsed (~100−150 ns for 10^{11} ppp beam intensity in phase-I and 50 ns for 10^{12} ppp beam intensity in phase-II) heavy ion beam will be available. Closed to BRing, the WDM terminal locates at the external experimental cave, where a Final Focus Lens system will be installed to strongly focus the beam to a small size (~1 mm FWHM). Finally, the high energy, focused and short pulsed heavy ion beam heats the target from a solid to the WDM and the relevant research will be performed. Table 1 shows the main parameters of the HIAF complex.

In order to foresee the state of WDM produced by the intense ion beam of HIAF, a two dimensional hydrodynamic compute code BIG-2 has been done by Dr. N. Tahir under the collaboration. The BIG-2 code is based on a Godunov-type scheme that has a second-order accuracy in space for solving the hydrodynamic equations. It uses rectangular grids and includes heat conduction and applies EOS data in tabular form or others. It also includes energy deposition by the projectile ions with the beam geometry taking into account [27,28].

Table 1
Main parameters of HIAF-I.

	Ion species	Beam energy	Beam intensity
SECR	$^{238}U^{34+}$	14 keV/u	0.05 pmA
iLinac	$^{238}U^{34+}$	17 MeV/u	0.028 pmA
BRing	$^{238}U^{34+}$	0.8 GeV/u	~1.4 × 10^{11} ppp
SRing	Radioactive ions	0.84 GeV/u	~10^{9-10} ppp
	fully stripped, H−, He-like	0.8 GeV/u	~10^{11-12} ppp
MRing	$^{238}U^{92+}$	0.8 GeV/u	~10^{11} ppp

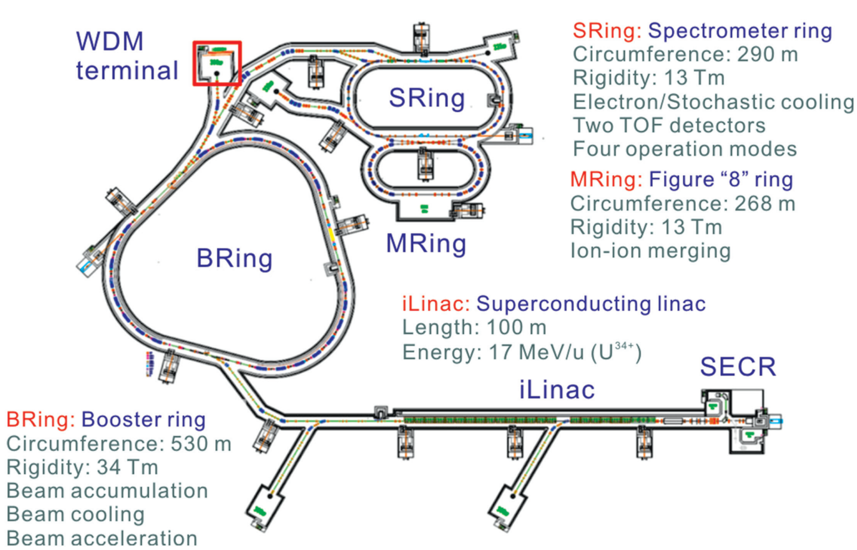

Fig. 1. Schematic view of the HIAF complex. The facility of HIAF includes SECR, iLinac, BRing, SRing, MRing, FRS beam lines and serveral experimental terminals at low-, intermediate-, and high-energy sections. The relevant paramters of each parts are indicated. The WDM terminal locates at the external experimenal cave of BRing.

The thermodynamic and hydrodynamic responses of a solid lead cylindrical target heated by $^{238}U^{34+}$ ions accelerated by the BRing are studied. We consider a $^{238}U^{34+}$ ion beam with an energy of 800 MeV/u, a bunch length of 100−150 ns with a Gaussian intensity distribution along the radius characterized with FWHM = 1 mm. The beam intensity is $N = 1 \times 10^{11}$ ppp. The target is a solid cylinder having a length of $L = 5$ mm and a radius of $r = 4$ mm. The beam is incident over one face of the target and the projectiles penetrate into the target. The range of 800 MeV/u uranium ions in the solid lead is about 1 cm, which is larger than the target length. Thus the energy is uniformly deposited along the cylinder length as the Bragg peak lies out of the target.

Fig. 2 shows the simulation result of the specific deposited-energy vs the radius at a longitudinal position of $L = 2.5$ mm (middle of the target) at different time (a), the case for temperature (b), pressure (c), and density (d), respectively.

It is seen that at $t = 150$ ns (end of the bunch), a maximum deposited-energy of ~14 kJ/g at the axis is achieved, where the temperature is ~55,000 K. The high temperature leads to a high pressure that drives a radially outgoing shock wave. The maximum pressure at the axis is about 65 GPa at $t = 100$ ns. An outward propagation of the shock wave is visible and the maximum density of the shocked region is ~14 g/cm^3.

Table 2 presents the maximum values of the target's physical parameters at the axis at the end of the bunch for different bunch lengths. All these calculations therefore suggest that the ion beam generated by the BRing of HIAF facility with these parameters is very suitable for generating WDM in laboratory. It is concluded that one can do some interesting experiments on WDM including the equation of state, generation of plane shock waves and related problems of interest.

Table 2
Physical states of the lead target which is heated by 800 MeV/u $^{238}U^{34+}$ ion beams with different pulse lengths impact on the lead target.

	50 ns	100 ns	150 ns
E (kJ/g)	15.3	14.8	14.0
p (GPa)	91.0	75.0	58.0
T (K)	60,000	58,000	55,000
ρ (g/cm^3)	11.0	10.2	9.3

3. Diagnostics for WDM research

3.1. High energy electron radiography

For a fast dynamic process, diagnostics of the spatial, density and element distributions of a bulk target and their evolution are of key importance. Apart from the imaging with self-radiation, like X-ray or neutrons from the target, high energy proton or electron radiography shows some advantages, in particular as it ensures the long penetration distance, high spatial resolution, large dynamic range, high sensitivity to the density and material element [24,29−34]. The high energy

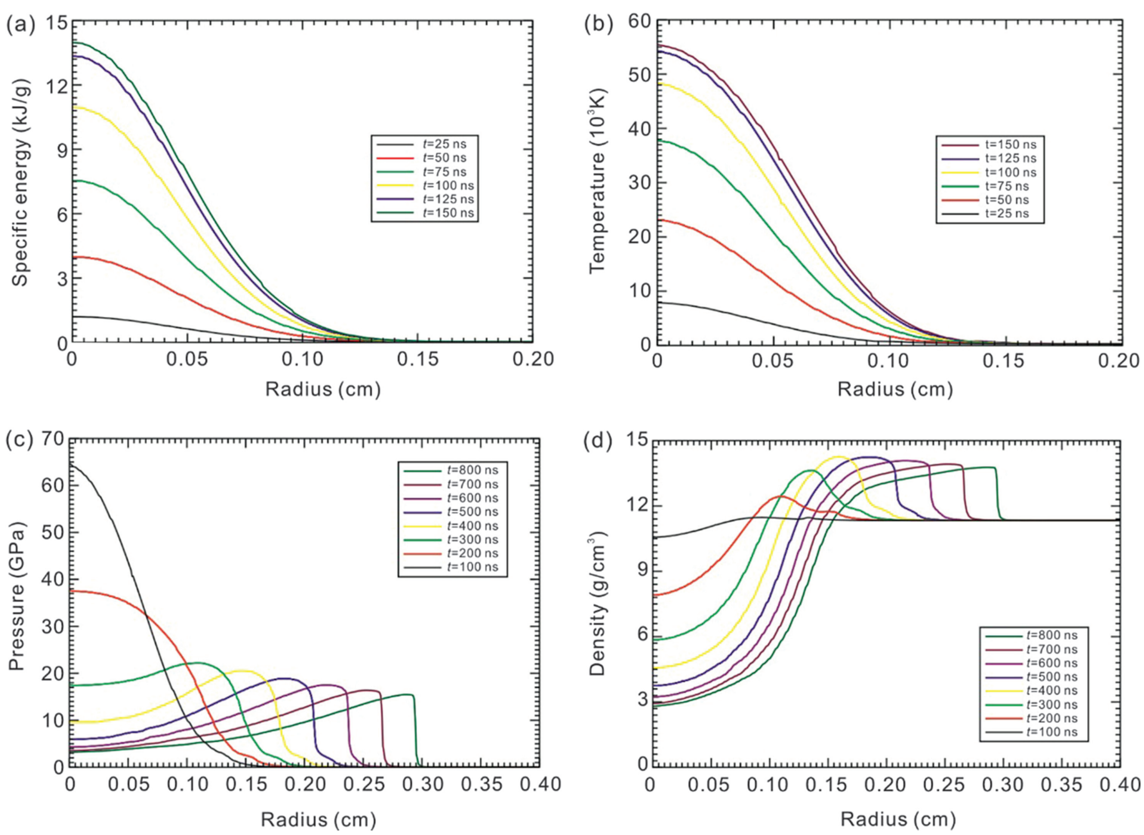

Fig. 2. Specific depsotited-energy vs. target radius at (a) $L = 2.5$ mm of the longitudinal position in a cylindrical lead target, which is heated by 800 MeV/u $^{238}U^{34+}$ ions with a bunch length of 150 ns and a beam size of 1 mm. (b) The temperature, (c) pressure and (d) density vs. radius are shown, respectively.

proton radiography [35−37] has been proposed by Los Alamos National Laboratory (LANL) and it experimentally shows the potential for WDM diagnostics with high spatial and temporal resolution [38]. In FAIR project, a 4.5 GeV proton beam is proposed to diagnose the state of high-energy-density matter [39,40].

However, a high energy proton accelerator is very costly and large in size. A ps-scale proton beam bunch with desired energy and intensity for ultra-fast radiography is not available yet in laboratory. High energy electron radiography (HEER) has become one of the important candidates at IMP with the collaboration of Tsinghua University (THU), China and Argonne National Laboratory, USA, who proposed the high energy electron radiography aiming to be applied in the diagnose of WDM at HIAF [41,42]. A principle experiment has been done and the high quality electron beams were extracted from THU e-LINAC accelerator based on radio frequency photocathode gun and s-band technology. The beams with an energy of 50 MeV, bunch length of 1 ps and bunch intensity ranging from a few pC to 100 nC, beam emittance of ~2 mm-mrad and beam spot size ~3 mm, were used in the experiment. In order to systematically investigate the high energy electron radiography further, the group of IMP newly designed and constructed a special beam line at THU e-LINAC facility. Fig. 3 (a) shows the new beam line. A linear achromat, consists of two rectangular dipoles and three quadrupoles, is used for deflecting the beam by 90° because of the limited space in laboratory. The target is placed after the achromat at the object plane position. The imaging system is after the target. Two kinds of imaging systems are designed with different magnification factor, with symmetric doublet and triplet quadrupoles, as well as the aperture placed at the Fourier plane position. Fig. 3 (b) shows the parameters of the imaging lattice with different magnification factors.

We take a TEM grid (material: Mo) which has 200 lines/inch with a hole width of 90 μm, bar width of 35 μm, thickness of 25 μm and diameter of 3 mm, as the target to measure the spatial resolution. At the imaging plane, the radiography picture is obtained. It is seen that a very clear grid structure and the spatial resolution are measured as 6.5 μm. Noted that such a radiography picture is produced by one shot of a bunch of electrons (shown in Fig. 4).

We obtain the electron radiography by applying a 0.8 mm thick silicon target (two pieces of Si wafers stacked up with one rotated 90°) with a stepwise structure as the imaging object too (shown in Fig. 5). The very apparent stepwise structure is correlated to the real target and the luminescence intensity at different steps agrees with its depth in the target well.

The principle experiment of high energy picosecond pulse-width electron bunch radiography proves that the kind of e-LINAC and picosecond bunch length electron can be applied in the research of WDM. The properties of high spatial resolution about a few microns and high sensitivity of density, as well as the picosecond-scale temporal resolution can fulfill the requirements of diagnosing a dynamic process of WDM.

In order to make a better diagnostic by using the electron radiography, a new RF type high energy electron LINAC accelerator complex is under construction at IMP, Lanzhou, which will carry out the systematically experimental radiography investigations. The new electron linac structure is shown in Fig. 6. Both radio frequencies accelerated thermionic

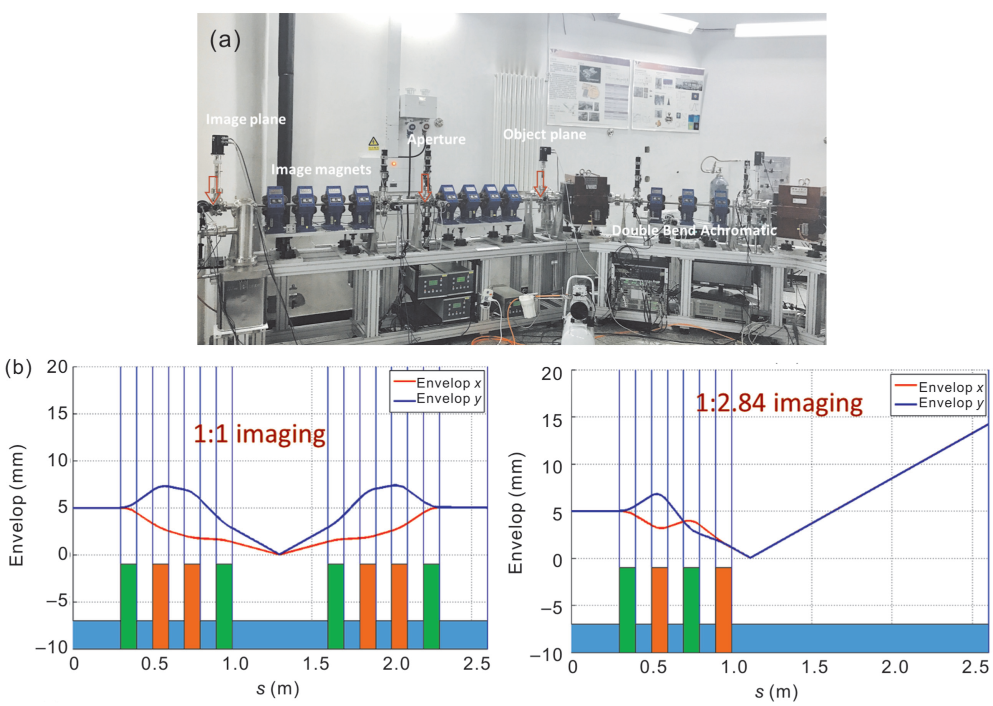

Fig. 3. (a) Newly designed and constructed beam line for high energy electron radiography research at THU e-LINAC by IMP and (b) the parameters of the imaging lattice with different magnification factors.

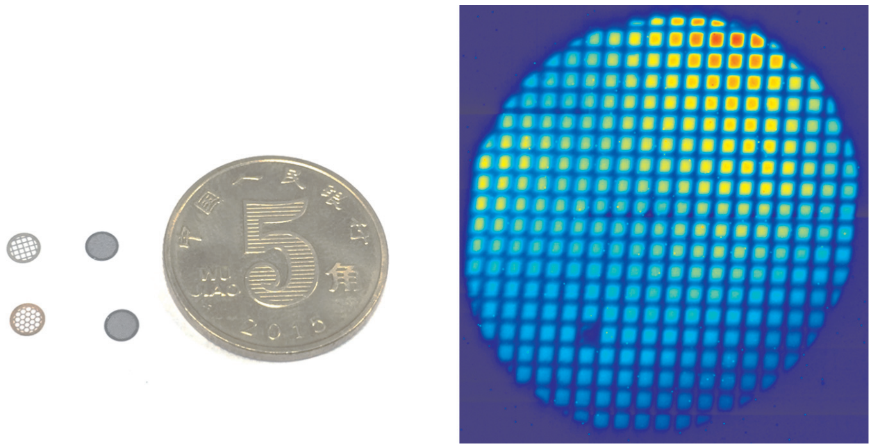

Fig. 4. TEM grid samples of high energy electron radiography research and the obtained results by applying 44 MeV, 1 ps pulse width and 300 pC intensity electron beam impact on the sample at THU.

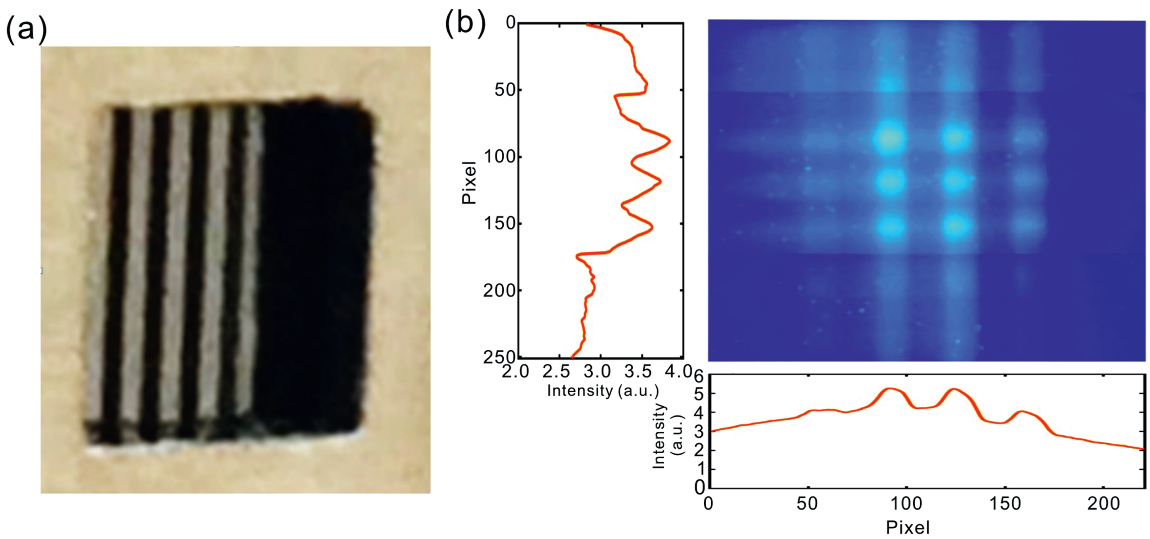

Fig. 5. (a) Picture of one piece of the step Si wafer. In our experiment, two step wafers stacked up with a total thickness of 0.8 mm compose a new stepwise target with one rotated 90° from the other. (b) The radiograph and measured luminescence intensities along the two vertical directions. The grid characteristic correlated to the structure of the stacked stepwise target can be seen in the radiograph.

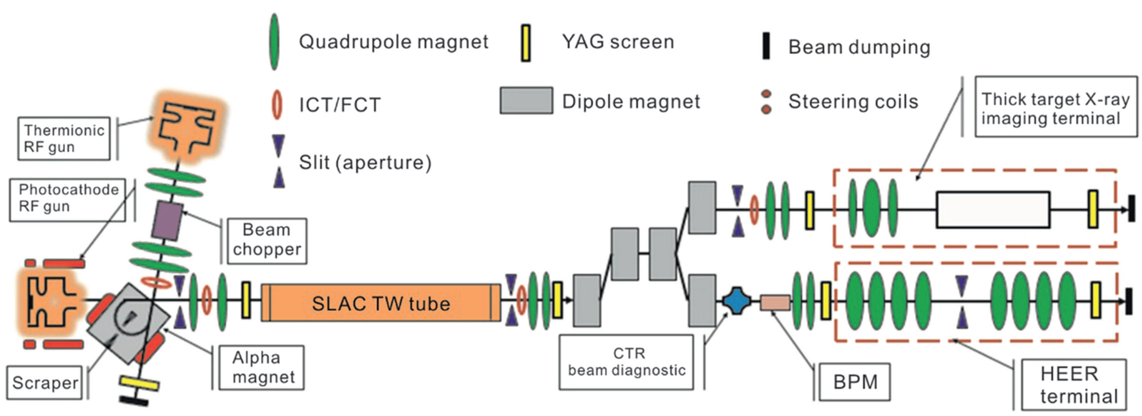

Fig. 6. New HEER platform under construction at IMP, where both RF thermionic cathode type and photocathode type electron guns will be employed. X-ray imaging induced by the electron beam will be available too.

cathode type and photocathode type electron beams with an energy of 60 MeV are simultaneously developed at the new platform and the X-ray imaging besides HEER will be available too. The energy of 60 MeV is chosen because of the physical structure, designed parameters and the budget. Based on the results obtained from THU electron accelerator, 60 MeV is good enough to carry out the radiography experiments on a solid target (thickness about 1 mm). And ~10 μm spatial resolution can be achieved. If we use a larger magnification lens system to zoom in the target, higher spatial resolutions are expected to be obtained. In the future, the electron beams with ~800 MeV will be built to diagnose the WDM (even 10 times of the solid density) at HIAF and the spatial resolution can be better than 10 μm.

3.2. New design of a fast multi-channel pyrometer

Temperature as one of the key parameters of WDM, is highly required in a dynamic process measurement with the properties of fast and highly accurate. A new designed fast multi-channel pyrometer was proposed by analyzing the Planckian emission spectra in ultraviolet, visible and infrared spectral regions, respectively, with a very high frequency when the intense heavy ion beam impacts on a target and the evolution of target temperature can be obtained. A six-channel pyrometer has been developed at GSI and a test experiment using U^{74+} ion beams to impact on tungsten foils is reported in Ref. [43].

Fig. 7 shows the working scheme of a newly-developed eight-channel pyrometer on the basis of Planck black-body radiation. The narrow-band interference filters which play the role of filtering and reflection, separate the import light transmitting by optical fiber to 8 channels, from 500 nm to 1500 nm. The high working frequency (30 kHz−1 GHz) photodiodes (Si type and InGaAs type) are used and a very fast rise time about 500 ps can be achieved. A high spatial resolution of the pyrometer is realized through the optical fibers (400 μm diameter) array in the optical collection closely facing to the target. With more paths of light and fast detectors, a broad range (1,500−20,000 K) of temperature can be diagnosed more accurately. This multi-channel pyrometer will serve the temperature diagnosis for WDM research at HIAF.

Fig. 8 shows the result of a testing experiment measured by a pyrometer of the plasma intensity changing with time in 10 ns duration and 300 mJ at 532 nm laser shot on a solid lead target. We recorded the light intensity change with time from different channels (500 to 1500 nm). The duration of the light is ~1000 ns, which agrees with the lifetime of the laser induced plasma. Next we will calibrate the pyrometer by using a standard light source to obtain the temperature information.

3.3. In-situ diagnostics of ions energy loss and charge state

At the HIAF, the WDM will be generated by the energy deposition of heavy ions when they are travelling in the target. Thus the energy loss process of ions in matter is of key importance to determine the final state of WDM. Moreover, theoretical prediction and experimental result show that the energy loss process of heavy ions in warm dense matter may be quite different because of the strong coupling effect comparing to cold matter [44,45]. Simultaneously the ions charge state will increase due to the suppression of

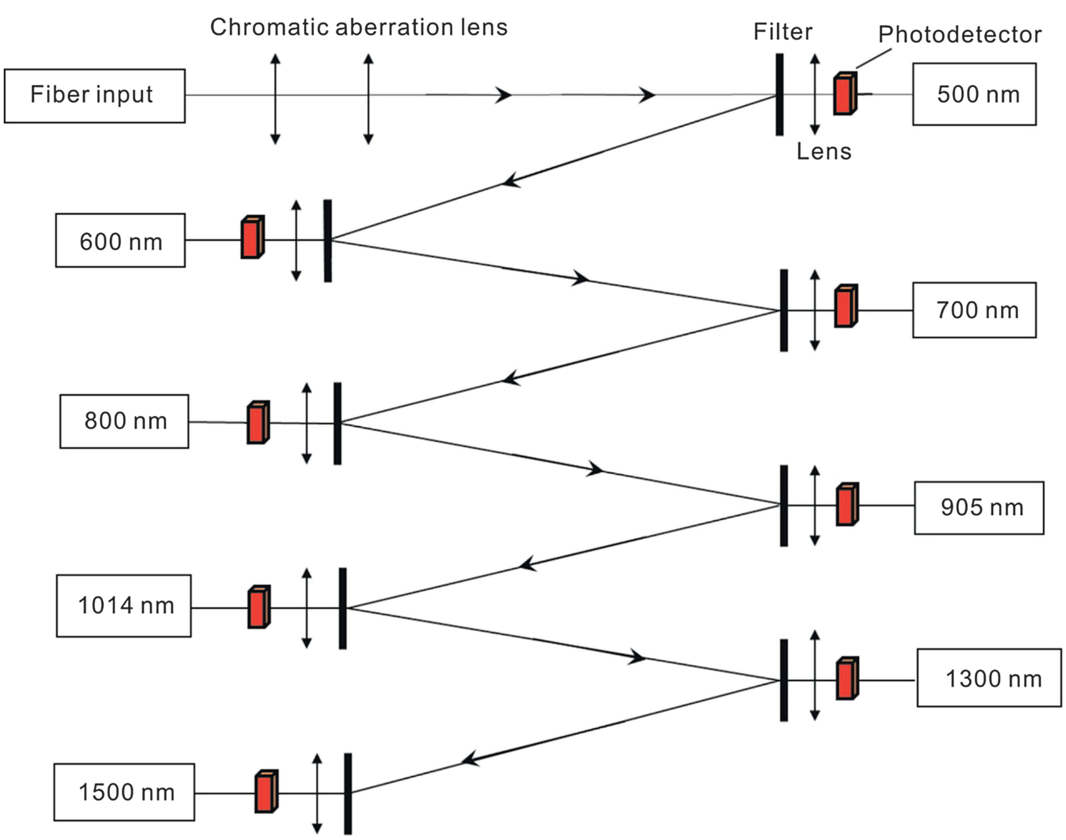

Fig. 7. Working scheme of the newly-developed 8-channel pyrometer.

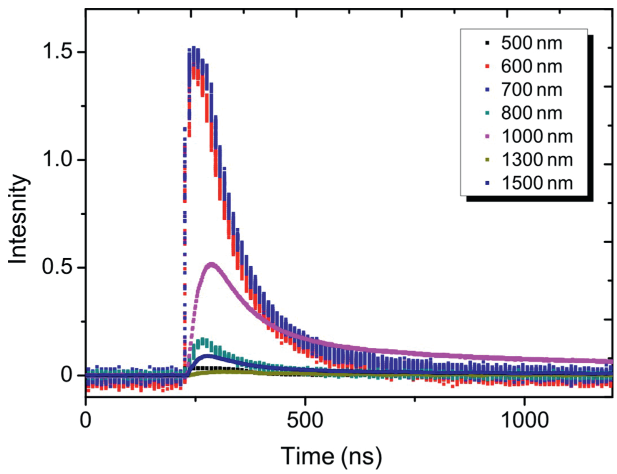

Fig. 8. Intensity changes with time from different channels (500 to 1500 nm) and the plasmas produced by a 10 ns duration, 300 mJ@532 nm laser shot on a lead target measured by a pyrometer.

recombination process [46,47]. Therefore, an in-situ diagnostic of the energy loss and charge state for heavy ions in warm dense matter are developed.

Fig. 9 shows schematically the in-situ detector system. The well-focused intense heavy ion beams impact on the target to generate WDM and the outgoing ions are collimated to fly in a drift area where a strong dipole magnetic field is available. Without dipole magnet-function 1, the ions will penetrate into a scintillator and stop inside. The light emission along the trajectory will be induced and the areal fluorescence intensity is proportional to the energy deposition rate. At the end of the range, a relative higher intensity, the so-called Bragg peak, which has a very sharp spatial edge (around several tens of microns), exists. An optical lens focuses at the Bragg peak and a high spatial resolution CCD camera will be used to record the result. One can easily determine the energy of ions by measuring the Bragg peak position due to the strong contrast for Bragg peak in the image. Based on the HIRFL facility, we have made the experiments by using CsI(Tl) scintillator, a CCD camera and coupled optical lens to in-situ diagnose the energies of 100−150 MeV/u carbon ions. The energies determined by the positions of the Bragg peak were compared with the results of LISE calculation and it is found that the accuracy of energy could be about 1%. Moreover, we have proposed a new method to increase the energy resolution through applying the optical filter to identify the fluorescence from projectiles themselves against the light from secondary particles and to increase the spatial resolution at the Bragg peak position. A recent experiment has shown that the light spectrum from CsI (Tl) scintillator of ions induced is different from the case of X-ray induced, and a characteristic peak for ions was found at about 377 nm wavelength [48]. Thus a narrow-band optical filter in front of the photodiode will be used to distinguish the position of Bragg peaks more clearly. As a result, a higher energy resolution of the detector system can be obtained.

Fig. 10 shows schematically the newly developed Bragg peak detector. An ICCD camera focused at the scintillator at 90° is employed to monitor the ions trajectory and a similar work has been reported in Ref. [49]. The additional optical array and filters are used to transmit the effective light which is mainly from the projectiles to the photodetectors and to clearly distinguish the Bragg peak position.

By applying the dipole magnet-function 2, the different charge state ions lie at different positions of the scintillator and are recorded by the ICCD camera. According to the measured energy of ions, the magnet field and drift length, the charge states of ions are diagnosed.

4. Summary and outlook

In the article, we report the new accelerator facility HIAF in China. The state of matter generated by uranium ions from BRing of HIAF impacting on a lead cylinder target is simulated and the result shows that the state with temperature about 55,000 K, pressure ~60 GPa and remaining in solid density can be achieved. The new opportunities of heavy ion beam-driven WDM research can be seen. In order to more precisely diagnose the WDM state, we introduce some newly developed diagnostic techniques. The high energy electron radiography has shown some prior advantages: long inspection range for

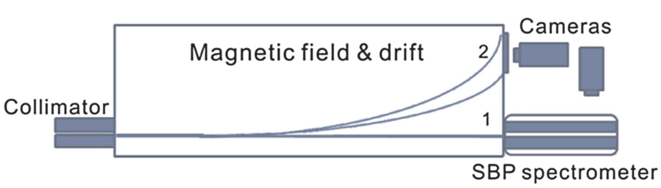

Fig. 9. Schematic view of the energy loss and charge state detector system.

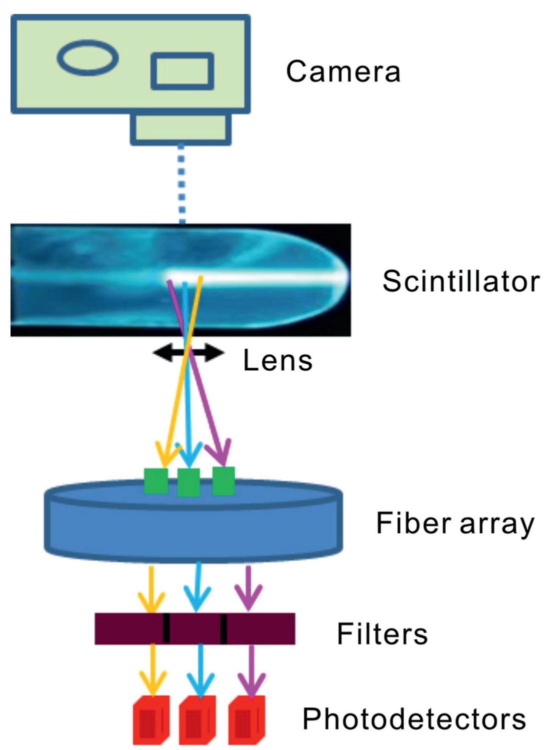

Fig. 10. Scheme of the developed scintillating Bragg-peak detector.

thick target, high spatial resolution of a few microns, high sensitivity of areal density, ultrafast temporal resolution of 1−10 ps by applying the RF photocathode technique. A new 8-channel pyrometer was developed to diagnose the temperature of WDM, which measured the light wavelength from 500 nm to 1500 nm and temperature range of 1,500 K to 20,000 K. Considering the importance of energy deposition to generate a WDM in the research of heavy ions beam driven, an in-situ energy loss and charge state of ion detector system were introduced. By precisely measuring the Bragg peak position in the scintillator and the spatial distribution of ions in a dipole magnet field, the energy and charge states of ions can be obtained. Our recent experiment shows that a characteristic peak exists in the light spectrum induced by heavy ions impact on CsI(Tl) scintillator, which may increase the spatial resolution of Bragg peak and improve the energy resolution of the detector system.

So far the design on the accelerator complex has been accomplished, the important physical platform has been created and the HIAF will go into civil construction soon. However, the physical and technical details on WDM terminal are still under discussion, and new ideas and important comments on WDM investigation at HIAF are very welcome.

Conflict of interest

The authors declare that there is no conflicts of interest.

Acknowledgement

This work was supported by the National Science Foundation of China (NSFC, Grant Nos. U1532263, 11205225, 11275241, 11375034, 11505248 and 11275238). We thank D. Hoffmann, N. Tahir, R. Piriz and the HIAF committee at IMP.

References

[1] R.C. Davidson, Frontiers in High Energy Density Physics, National Research Council of the National Academies, National Academies Press, Washington, DC, USA, 2003.
[2] R.W. Lee, D. Kalantar, J. Molitoris, Warm Dense Matter: An Overview, 2004 in Livemore, UCRL-TR-203844.
[3] G.W. Collins, L.B. Da Silva, P. Celliers, D.M. Gold, M.E. Foord, et al., Measurements of the equation of state of deuterium at the fluid insulator-metal transition, Science 281 (1998) 1178.
[4] N.A. Tahir, A. Shutov, A.R. Piriz, Th. Stöhlker, High energy density physics research using intense heavy ion beam at FAIR: the HEDgeHOB program, J. Phy.: Conference Series 688 (2016) 012118.
[5] D.H.H. Hoffmann, V.E. Fortov, M. Kuster, V. Mintsev, B.Y. Sharkov, et al., High energy density physics generated by intense heavy ion beams, Astrophy Space Sci. 322 (2009) 167.
[6] Y.T. Zhao, R. Cheng, Y.Y. Wang, X.M. Zhou, Y. Lei, et al., Heigh energy density physics research at IMP, Lanzhou, China, High Power Laser Science and Engineering 2 (2014) e39.
[7] P. Renaudin, C. Blancard, G. Faussurier, P. Noiret, Combined pressure and electrical-resistivity measurements of warm dense aluminum and titanium plasmas, Phys. Rev. Lett. 88 (2002) 215001.
[8] I. Krisch, H.J. Kunze, Measurements of electrical conductivity and mean ionization state of nonideal aluminum plasmas, Phys. Rev. E 58 (1998) 6557.
[9] S. Saleem, J. Haun, H.-J. Kunze, Electrical conductivity measurements of strongly coupled W plasmas, Phys. Rev. E 64 (2001) 056403.
[10] T. Sasaki, M. Nakajima, T. Kawamura, K. Horioka, Semi-empirical approach to pulsed wire discharges in water as a method for warm dense matter studies, J. Plasma Fusion Res. 81 (12) (2005) 965.
[11] T. Sasaki, Y. Yano, M. Nakajima, T. Kawamura, K. Horioka, Evaluation of copper conductivity in warm dense state using exploding wire in water, Laser Part. Beams 24 (2006) 371, Prog. Nucl. Energy 50 (2008) 611.
[12] H. Yoneda, H. Morikami, K. Ueda, R.M. More, Ultrashort-pulse laser ellipsometric pump-probe experiments on gold targets, Phys. Rev. Lett. 91 (2003) 075004.
[13] S.H. Glenzer, G. Gregori, F.J. Rogers, D.H. froula, S.W. Pollaine, R.S. Wallace, X-ray scattering from solid density plasmas, Phys. Plasma. 10 (2003) 2433.
[14] S.H. Glenzer, O.L. Landen, P. Neumayer, R.W. Lee, K. Widmann, et al., Observations of plasmons in warm dense matter, Phys. Rev. Lett. 98 (2007) 06500.
[15] D.H.H. Hoffmanna, A. Blazevic, S. Korostiy, P. Ni, S.A. Pikuz, et al., Inertial fusion energy issues of intense heavy ion and laser beams interacting with ionized matter studied at GSI-Darmstadt, Nucl. Instrum. Meth. A 577 (2007) 8−13.
[16] B.G. Logan, F.M. Bieniosek, C.M. Celata, J. Coleman, W. Greenway, et al., Recent US advances in ion-beam-driven high energy density physics and heavy ion fusion, Nucl. Instrum. Meth. A 577 (2007) 1−7.
[17] S. Kawataa, K. Horiokab, M. Murakamic, Y. Ogurib, J. Hasegawab, et al., Studies on heavy ion fusion and high energy density physics in Japan, Nucl. Instrum. Meth. A 577 (2007) 21−29.
[18] W.F. Henning, The future GSI facility, Nucl. Instrum. Meth. B 214 (2004) 211.
[19] B.Yu. Sharkov, Overview of Russian heavy-ion inertial fusion energy program, Nucl. Instrum. Meth. A 577 (2007) 14−20.
[20] M. Roth, T.E. Cowan, M.H. Key, S.P. Hatchett, C. Brown, et al., Fast ignition by intense laser-accelerated proton beams, Phys. Rev. Lett. 86 (2001) 436.
[21] H. Qin, R.C. Davidson, B.G. Logan, Centroid and envelope dynamics of high-intensity charged-particle beams in an external focusing lattice and oscillating wobbler, Phys. Rev. Lett. 104 (2010) 254801.
[22] N.A. Tahir, Th. Stöhlker, A. Shutov, I.V. Lomonosov, V.E. Fortov, et al., Ultrahigh compression of water using intense heavy ion beams: laboratory planetary physics, N. J. Phys. 12 (2010) 073022.
[23] F. Genco, A. Hassanein, Particle-in-cell methods in predicting materials behavior during high power deposition, Laser Part. Beams 32 (2014) 217.
[24] Y.T. Zhao, Z.H. Hu, R. Cheng, Y.Y. Wang, H.B. Peng, et al., Trends in heavy ion interaction with plasma, Laser Part. Beams 30 (2012) 679−706.
[25] X.W. Ma, W.Q. Wen, S.F. Zhang, D.Y. Yu, R. Cheng, et al., HIAF: New opportunities for atomic physics with highly charged heavy ions, Nucl. Instr. Meth. B 408 (2017) 169.
[26] J.C. Yang, J.W. Xia, G.Q. Xiao, H.S. Xu, H.W. Zhao, et al., High intensity heavy ion accelerator facility (HIAF) in China, Nucl. Instrum. Meth. B 317 (2013) 263.
[27] N.A. Tahira, A. Adoninb, C. Deutschc, V.E. Fortovd, N. Grandjouane, et al., Studies of heavy ion-induced high-energy density states in matter at the GSI Darmstadt SIS-18 and future FAIR facility, Nucl. Inst. Meth. Phys .Res. A 544 (2005) 16−26.
[28] V.E. Fortov, B. Goel, C.-D. Munz, A.L. Ni, A. Shutov, et al., Numerical simulation of nonstationary fronts and interfaces by the Godunov method in moving grids, Nucl. Sci. Eng. 123 (1996) 169.
[29] L.N. Sheng, Y.T. Zhao, G.J. Yang, T. Wei, X.G. Jiang, et al., Heavy-ion radiography facility at the institute of modern physics, Laser Part. Beams 32 (2014) 651.
[30] N.S.P. King, E. Ables, Ken Adams, K.R. Alrick, J.F. Amann, An 800-MeV proton radiography facility for dynamic experiments, Nucl. Instrum. Meth. A 424 (1999) 84−91.
[31] D. Varentsov, O. Antonov, A. Bakhmutova, A. Bogdanov, C.R. Danly, et al., Commissioning of the PRIOR Prototype, GSI Scientific Report, APPA-MML-PP-02, 2014, pp. 275−276.
[32] C.K. Li, F.H. Séguin, J.R. Rygg, J.A. Frenje, M. Manuel, et al., Monoenergetic-proton-radiography measurements of implosion dynamics in direct-drive inertial-confinement fusion, Phys. Rev. Lett. 100 (2008) 225001.

[33] F.E. Merrill, Imaging with penetrating radiation for the study of small dynamic physical processes, Laser Part. Beams 33 (2015) 425−431.
[34] F.E. Merrill, E. Campos, C. Espinoza, G. Hogan, B. Hollander, et al., Magnifying lenses for 800 MeV proton radiography, Rev. Sci. Instrum. 82 (2011) 103709.
[35] D. Varentsov, O. Antonov, A. Bakhmutova, C.W. Barnes, A. Bogdanov, et al., Commissioning of the PRIOR proton microscope, Rev. Sci. Instrum. 87 (2016), 023303/1−023303/8.
[36] A.V. Kantsyrev, A.A. Golubev, V. Bogdanov, V.S. Demidov, E.V. Demidova, et al., TWAC-ITEP proton microscopy facility, Instrum. Exp. Tech. 57 (2014) 1−10.
[37] Yu. M. Antipov, A.G. Afonin, A.V. Vasilevskii, I.A. Gusev, V.I. Demyanchuk, et al., A radiographic facility for the 70 GeV proton accelerator of the institute for high energy physics, Instrum. Exp. Tech. 53 (2010) 319−326.
[38] F. Merrill, F. Harmon, A. Hunt, F. Mariam, K. Morley, et al., Electron radiography, Nucl. Instrum. Meth. B 261 (2007) 382−386.
[39] F.E. Merrill, A.A. Golubev, F.G. Mariam, V.I. Turtikov, D. Varentsov, Proton microscopy at FAIR, AIP Conf. Proc. 1195 (2009) 667−670.
[40] D. Varentsov, A. Bogdanov, V.S. Demidov, A.A. Golubev, A. Kantsyrev, et al., First biological images with high-energy proton microscopy, Phys. Med. 29 (2013) 208−213.
[41] Y. Zhao, Z.M. Zhang, W. Gai, Y. Du, S. Cao, et al., High energy electron radiography scheme with high spatial and temporal resolution in three dimension based on a e-LINAC, Laser Part. Beams 34 (2016) 338−342.
[42] Q.T. Zhao, S.C. Cao, M. Liu, X.K. Sheng, Y.R. Wang, et al., High energy electron radiography system design and simulation study of beam angle-position correlation and aperture effect on the images, Nucl. Instrum. Meth. A 832 (2016) 144−151.
[43] P.A. Ni, M.I. Kulish, V. Mintsev, D.N. Nikolaev, V.Ya. Ternovoi, et al., Temperature measurement of warm-dense-matter generated by intense heavy-ion beams, Laser Part. Beams 26 (2008) 583−589.
[44] J.C. Deng, Y.T. Zhao, R. Cheng, X.M. Zhou, H.B. Peng, et al., Investigation on the energy loss in low energy protons interacting with hydrogen plasma, Acta Phys. Sin. 64 (2015) 145202.
[45] A.B. Zylstra, J.A. Frenje, P.E. Grabowski, C.K. Li, G.W. Collins, et al., Measurement of charged-particle stopping in warm dense plasma, Phys. Rev. Lett. 114 (2015) 215002.
[46] D. Gericke, M. Schlanges, Beam-plasma coupling effects on the stopping power of dense plasmas, Phys. Rev. E 60 (1999) 904.
[47] G. Zwicknagel, C. Toepffer, P.-G. Reinhard, Stopping power in highly correlated plasmas, Phys. Rep. 309 (1999) 117.
[48] D. Varentsov, Energy Loss Dynamics of Intense Heavy Ion Beams Interacting with Dense Matter, Ph.D. thesis, Technische Universität Darmstadt, 2002.
[49] Y. Lei, Y.T. Zhao, R. Cheng, X.M. Zhou, Y.B. Sun, et al., Fluorescence emission from CsI(Tl) crystal induced by high-energy carbon ions, Opt. Mater. 35 (2013) 1179−1183.